inorganics

MDPI

Article

Transition Metal Complexes of Schiff Base Ligands Prepared from Reaction of Aminobenzothiazole with Benzaldehydes

Mahmoud Sunjuk [1,*], Lana Al-Najjar [1], Majed Shtaiwi [1], Bassam El-Eswed [2], Mousa Al-Noaimi [1,3], Luay Al-Essa [4] and Kamal Sweidan [5]

[1] Department of Chemistry, Faculty of Science, The Hashemite University, Zarqa 13133, Jordan; lanam_s@hu.edu.jo (L.A.-N.); MajedH@hu.edu.jo (M.S.); manoaimi@hu.edu.jo (M.A.-N.)
[2] Department of Basic Sciences, Zarqa College, Al-Balqa Applied University, Al Salt 19117, Jordan; bassameswed@bau.edu.jo
[3] Chemistry Department, Faculty of Science, Kuwait University, Safat 13060, Kuwait
[4] Department of Pharmacy, Faculty of Pharmacy, Al-Zaytoonah University of Jordan, Amman 11733, Jordan; luayyousif@yahoo.com
[5] Department of Chemistry, The University of Jordan, Amman 11942, Jordan; k.Sweidan@ju.edu.jo
* Correspondence: Mahmoud.Sunjuk@hu.edu.jo

Abstract: Schiff bases have played significant roles in the development of inorganic or coordination chemistry. Three Schiff base (NB, CB and HB) ligands, prepared for the reaction of 2-amino-6-methoxy-benzothiazole with 2-Nitrobenzaldehyde, 2-chlorobenzaldehyde and 2,4-Dihydroxybenzaldehyed, respectively, were investigated for their transition metal complexes, which were prepared by reacting the ligand (2:1 molar ratio) with Co(II), Ni(II), Cu(II), Cd(II), Cr(III) and Fe(III) chlorides. The nature of the interaction between the metal ions and ligands (L) was studied with the aid of magnetic susceptibility, elemental analysis, FTIR and ^{1}H-NMR spectroscopy. Based on the magnetic superstability and elemental analysis results, octahedral structures of the complexes, such as [ML_2Cl_2] or [$ML_2Cl(OH)$], were proposed for Cu(II), Cd(II), Co(II) and Ni(II) in which the ligand (L:NB, CB or HB) is bidentate through the azomethine and benzothiazole nitrogen. For Cr(III) and Fe(III) complexes, octahedral $ML_2Cl(OH)_2$ or $ML_2(OH)_3$ structures were proposed, where one ligand is monodentate and the other is bidentate. The azomethine ν(-HC=N-) and ^{1}H-NMR peaks of NB and CB were shifted to a higher frequency and downfield, respectively, upon complexation with metal ions. The bonding of OH groups of HB to Co(II), Cu(II) and Ni(II) enables π-backdonation from these metals to the azomethine of Schiff bases and the consequent shift of ν(-HC=N-) to a lower frequency and changes in the intensity of the ^{1}H-NMR peak of OH. On the other hand, this backdonation was not evidenced in the FTIR of HB complexes with high-charge Cr(III) and Fe(III) ions.

Keywords: Schiff bases; 2-amino-6-methoxy-benzothiazole; benzaldehyde; transition metal complexes

check for updates

Citation: Sunjuk, M.; Al-Najjar, L.; Shtaiwi, M.; El-Eswed, B.; Al-Noaimi, M.; Al-Essa, L.; Sweidan, K. Transition Metal Complexes of Schiff Base Ligands Prepared from Reaction of Aminobenzothiazole with Benzaldehydes. *Inorganics* **2022**, *10*, 43. https://doi.org/10.3390/inorganics10040043

Received: 1 March 2022
Accepted: 24 March 2022
Published: 30 March 2022

1. Introduction

Schiff bases are organic compounds that have a general formula of $R_1R_2C{=}NR'$ ($R' \neq H$), named by German chemist Hugo Schiff [1]. Schiff bases are usually synthesized from the condensation of an aliphatic or aromatic amine and carbonyl compound (aldehyde, ketone or acetyl compound) by nucleophilic addition. Aromatic Schiff bases are more stable than alkyl ones, and consequently, the former can be easily synthesized [2]. Schiff bases can be employed in many fields, including analytical, biological and as a ligand in inorganic chemistry [3]. Imine or azomethine groups ($R\text{-}CH{=}NR'$ where $R' \neq H$) are present in several natural and biologically active compounds [2]. Ancistrocladidine and *N*-salicylidene-2-hydroxyaniline are promising imine-based natural and synthetic molecules [4]. Furthermore, Schiff base amino acid complexes have special importance in inorganic chemistry due to their physiological and pharmacological activities [5]. Examples include the complexes of Co (II) with vitamin B12 and the complexes of Pd (II) with anticancer and antitumor agents [6].

At the present time, there is a great and growing interest in the binding of metal complexes with DNA, because this provides important information for new cancer therapeutic agents and potential probes for DNA structure and conformation. Hence, much attention has been focused on the design of metal-based complexes, particularly transition metal complexes, which can bind to or cleave DNA effectively [7].

The carbon-nitrogen double bond of Schiff bases, similar to the carbon-oxygen double bond, is readily reduced by metal complexes. Therefore, Schiff bases are versatile ligands, which coordinate to metal ions via nitrogen atoms located in azomethine [8]. Generally, Schiff bases are bi, tri or tetra-dentate chelate ligands and can form stable complexes with metal ions [9]. Thus, Schiff bases have played a significant role in the development of coordination chemistry and are involved as a key point in the development of inorganic biochemistry [3].

Schiff bases have a wide range of pharmacological effects and biological activities, including antibacterial, antimalarial, anti-inflammatory, antiviral and antipyretic properties, due to having an imine (-C=N-) linkage [10]. On the other hand, transition metal–Schiff base complexes have been found to possess certain biological and pharmacological properties such as antibacterial and antifungal activities [9,11].

Benzothiazoles, the precursors used in the present work, are found rarely in various marine or terrestrial natural compounds, which have useful biological activities. However, their derivatives are used in various branches of chemical research, for instance, in polymer chemistry, dyes, drugs and other fields [12]. 2-Substituted-1,3-benzothiazoles and their derivatives are part of bicyclic heteroaromatic compounds, which are widely used in many fields such as the medicine, pesticide and dye industries [13]. Recently, Schiff bases containing benzothiazole derivatives have been shown to have antimicrobial and antifungal activity [14].

The aim of the present work is to study the transition metal complexes of three Schiff base ligands (NB, CB and HB), which are prepared by the condensation of 2-amino-6-methoxybenzothiazol with 2-nitrobenzaldehyde, 2-chlorebenzaldehyde and 2,4-dihydroxybenzaldehyed, respectively (Scheme 1). The complexes with Cu(II), Co(II), Ni(II), Cd(II), Cr(III) and Fe(III) will be investigated for their spectroscopic properties, which include NMR and FTIR spectra, magnetic susceptibility and elemental compositions.

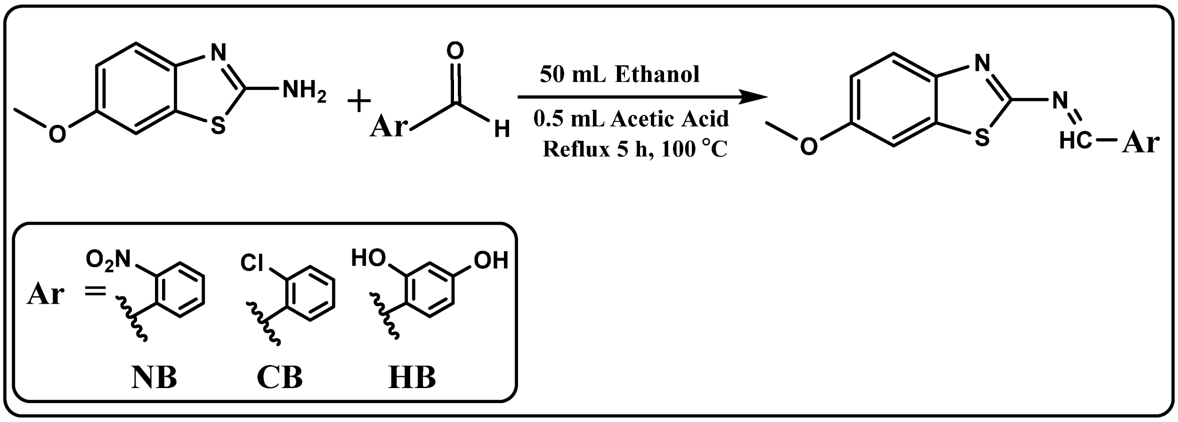

Scheme 1. Synthesis of Schiff bases ligands.

2. Results and Discussion

2.1. Synthesis of Schiff Bases Ligands

The ligands used in the present work were prepared previously using the same precursors and similar conditions [15–19]. The NB, CB and HB ligands (Scheme 1) were successfully synthesized with % yield ranges of 80 to 86%. The presence of either electron-withdrawing groups (NO_2 and Cl) or electron-donating groups (OH) on the aromatic aldehyde does not affect the % yield significantly. The colors of the ligands were yellow in the case of CB and HB and orange in the case of NB. The relatively high melting point of HB

(214–216 °C), which was much higher than that of NB (174–176 °C) and CB (122–124 °C), can be attributed to the strong H-bonding in the hydroxy-substituted HB.

The FTIR spectra of NB, CB and HB reflected the disappearance of sharp bands of the amine ν(NH2) at 3387 cm^{-1} found in the spectrum of 2-amino-6-methoxybenzothiazole and the appearance of stretching vibration of the azomethine group ν(-HC=N-) at 1606, 1602 and 1639 cm^{-1}, respectively. The nitro stretching vibrations ν(NO_2) at 1526 and 1349 cm^{-1} in the spectrum of 2-nitrobenzaldehyde shifted to a lower frequency at 1586 cm^{-1}, 1517 and 1337 cm^{-1}, respectively, upon formation of NB. Furthermore, the stretching vibrations of hydroxyl groups ν(C-OH) at 1494 and 1434 cm^{-1} in the spectrum of 2,4-dihydroxybensaldehyde were shifted to a lower frequency at 1472 and 1462 cm^{-1} in the case of HB. On the other hand, the stretching vibration of C-Cl at 753 cm^{-1} in the spectrum of 2-chlorobenzaldehyde was shifted to a higher frequency at 755 cm^{-1} in the case of CB.

The ^{1}H-NMR (400 MHz, DMSO-d^6) spectra of NB, CB and HB ligands showed two singlet peaks. The first was observed at δ = 3.86, 3.84 and 3.83 ppm, respectively, which was assigned to the methoxy group (-O-CH_3). The second peak at δ = 9.44, 9.42 and 9.17 ppm, respectively, were assigned to the azomethine proton (-HC=N-). The sets of peaks observed in the range of 6 to 8.5 ppm were ascribed to the aromatic rings. Two broad singlet peaks at δ = 10.68 ppm and δ = 12.01 ppm were attributed to the two hydroxyl protons of HB.

The ^{13}C-NMR resonances of the imine of benzothiazole ring (-C=N-) of NB, CB and HB occurred at δ = 168.3, 168.8 and 168.3 ppm, respectively, and the Schiff base azomethine carbon atom (-HC=N-) was observed at δ = 163.09 and 161.63 ppm, respectively. The peaks at δ = 56.24, 56.23 and 56.19 ppm, respectively, were assigned to the methoxy group (-O-CH_3). The peaks at δ = 145.9 and 136.8 ppm were assigned to carbon linked to the nitro group (-C-NO_2) and carbon linked to the chloride group (-C-Cl), respectively. The peaks at δ = 165.12 and 163.6 ppm were assigned to the two carbons linked to the hydroxyl groups (-C-OH). The unsubstituted aromatic carbons were observed in the range of 105 to 136 ppm.

2.2. *Synthesis of Metal Complexes*

The metal complexes were prepared following the procedures of [20] and [21] with some modifications, as shown in Scheme 2. The metal complexes were prepared by mixing a hot ethanolic solution of the Schiff base ligand (NB, CB and HB) with an ethanolic solution of the metal ion at a molar ratio of 2:1 and refluxing for 1 h. The resulting solution was concentrated by evaporating some of the solvent to precipitate the product, which was collected by suction filtration, then washed with cold ethanol and dried at 60 °C in a vacuum oven.

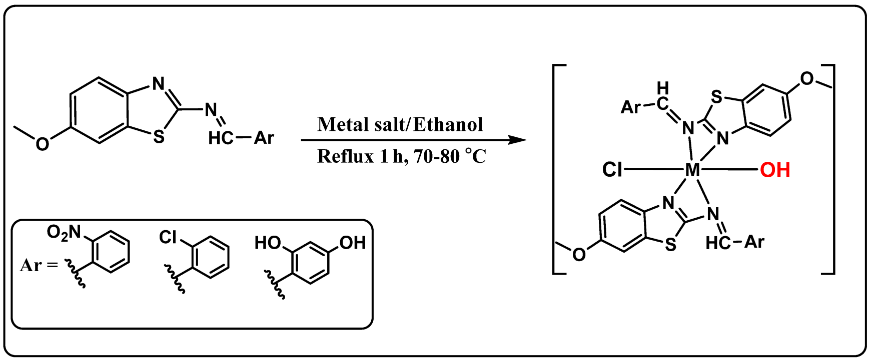

Scheme 2. Synthesis of metal complexes and their general structure. Detailed proposed structures are given in Section 3.3.1 depending on elemental analysis.

2.3. *Physical Properties of Complexes*

All the complexes have distinct colors from the free ligand except Cd-NB and Cd-HB. Remarkably, the melting points of HB complexes were much lower than that of the free HB ligand, except for Cd. Similarly, Cr-NB, Fe-NB, Cu-CB and Fe-CB have lower melting points than their corresponding ligands. Such low melting points may be due to either the hydroxyl or water molecules in the complexes (Section 3.3.1). The melting points of Cd-NB and Cd-HB are distinguished by their relatively high values. All metal complexes are insoluble in water, diethyl ether and petroleum ether but are soluble in ethanol, dimethylformamide and dimethyl sulfoxide.

2.4. Magnetic Susceptibility of Metal Complexes

The measured values of the magnetic moment (μeff, B.M) are given in Table 1. These values were compared with those of previously reported ranges and those expected from calculating the spin-only magnetic moment: (μ s.o. = $\sqrt{}$(S4(S + 1)) B.M.) where S = spin quantum number of unpaired electrons. The comparison with μ s.o. allows for predicting the orbital contribution to the magnetic moment, which is dependent on the electronic configuration of complexes. The observed magnetic moments of Cu-NB, Cu-CB and Cu-HB complexes were 1.88, 1.88 and 1.84 B.M, respectively, which agreed with the literature experimental range for Cu(II) octahedral complexes which is 1.7–2.2 B.M. [22,23] and μ s.o. (d^9, S = 1/2) = $\sqrt{}$(4(1/2) (1/2 + 1)) = 1.73 B.M. Similarly, the observed values of Cr-NB, Cr-CB and Cr-HB complexes (3.77, 3.73 and 3.87 B.M., respectively) were within the reported range for Cr(III) octahedral complexes, which is 3.7–3.9 [22] and μ s.o. (d^3, S = 3/2) = $\sqrt{}$(4(3/2) (3/2 + 1)) = 3.87. Furthermore, the observed values of Fe-NB, Fe-CB and Fe-HB complexes (6.01, 5.85 and 5.15 B.M., respectively) were within the reported range for high-spin Fe(III) octahedral complexes, which is 5.7–6.0 [22] and μ s.o. (d^5, S = 5/2) = $\sqrt{}$(4(5/2) (5/2 + 1)) = 5.92. Since the measured magnetic moments of Cu(II), Cr(III) and Fe(III) complexes agree with μ s.o., the orbital contribution to magnetic moment is minimal. This can be ascribed to the symmetrical occupation of the electronic configuration of t_2g in octahedral geometries [24,25].

Table 1. Magnetic susceptibility (B.M., Bohr Magnetons), of NB, CB and HB complexes.

Ligand	NB	CB	HB
Metal	**μeff (B.M)**	**μeff (B.M)**	**μeff (B.M)**
Cu	1.88	1.88	1.84
Cd	Dia	***	Dia
Cr	3.77	3.73	3.87
Fe	6.01	5.85	5.15
Co	4.84	5.28	5.73
Ni	***	3.37	2.90

*** Preparation of complexes was not successful.

The unsymmetrical t_2 occupation of electrons in tetrahedra Cu(II) and Cr(III) (e^4 $t_2{}^5$ and e^2 $t_2{}^1$, respectively) results in an orbital contribution to the magnetic moment [25], thus the tetrahedral geometry for Cu(II) and Cr(III) complexes may be not plausible. On the other hand, symmetrically occupied e^2 $t_2{}^3$ in a tetrahedral Fe(III) configuration does not possess orbital magnetism and, thus, tetrahedral geometry for Fe(III) complexes is possible. Using the same approach, the symmetrical electron occupation of (dxz, dyz) ($dx^2 - y^2$, dxy) (dz^2) in trigonal bipyramidal and (dxz, dyz) (dxy) (dz^2) ($dx^2 - y^2$) in square pyramidal Cu(II) and Fe(III) complexes implies the absence of orbital magnetism and, thus, these geometries may be possible. Furthermore, the unsymmetrical electron occupation $(dxz, dyz)^2$ $(dx^2 - y^2, dxy)^1$ in trigonal bipyramidal and symmetric electron occupation $(dxz, dyz)^2$ $(dxy)^1$ in square pyramidal Cr(III) complexes indicates that trigonal bipyramidal geometry is not possible, while square pyramidal geometry may be plausible.

The observed magnetic moments of Ni-CB and Ni-HB complexes (3.37 and 2.90 B.M., respectively) were in agreement with that reported for Ni(II) octahedral complexes (2.8–3.5) [22] and μ s.o. (d^8, S = 1) = $\sqrt{}$(4(1) (1 + 1)) = 2.83 B.M. The range in the literature for Ni(II) tetrahedral complexes, which is 4.2–4.8 [22], is far from our values, supporting an octahedral geometry for Ni(II). The higher magnetic moment for Ni(II) tetrahedral complexes is due to the unsymmetrical electron occupation in the tetrahedral e^4 $t_2{}^4$ Ni(II) configuration, which possesses an orbital contribution to the magnetic moment. Square planar geometry for Ni(II) complexes is excluded since it is diamagnetic [26,27]. The unsymmetrical electron occupation $(dxz, dyz)^4$ $(dx^2 - y^2, dxy)^3$ $(dz^2)^1$ in trigonal bipyramidal and symmetrical occupation $(dxz, dyz)^4$ $(dxy)^2$ $(dz^2)^1$ $(dx^2 - y^2)^1$ in square pyramidal Ni(II) complexes [28] reflect orbital magnetism in the former. Since no orbital contribution to the magnetic moment was observed in Ni(II) complexes, trigonal bipyramidal is not possible, while square pyramidal may be plausible.

The observed magnetic moments of Co-NB, Co-CB and Co-HB complexes (4.84, 5.28 and 5.73 B.M., respectively) were in agreement with that reported for Co(II) high-spin octahedral complexes (4.3–5.2) [22,29], but higher than the μ s.o. (d^7, S = 3/2) = $\sqrt{}$(4(3/2)(3/2 + 1)) = 3.87 B.M. Thus, an orbital contribution to the magnetic moment is expected due to the unsymmetrical electron occupation $t_{2g}{}^5$ $e_g{}^2$ in the high-spin octahedral Co(II) configuration. Symmetrical electron occupation in the tetrahedral e^4 $t_2{}^3$ Co(II) configuration has no orbital magnetism [24] and, consequently, tetrahedral geometry could be excluded. The range for Co(II) tetrahedral complexes in the literature, which is 4.2–4.8 [22], is far from our values, supporting the octahedral geometry for Co(II) complexes. Square planar geometry for Co(II) is very rare [28]. The symmetrical electron occupation $(dxz, dyz)^4$ $(dx^2 - y^2, dxy)^2$ $(dz^2)^1$ in trigonal bipyramidal and $(dxz, dyz)^4$ $(dxy)^1$ $(dz^2)^1$ $(dx^2 - y^2)^1$ in square pyramidal Co(II) complexes [28] implies no orbital magnetism. Since an orbital contribution to the magnetic moment was observed in Co(II) complexes, these geometries are not plausible. As expected, the Cd(II) complexes in Table 1 were diamagnetic [30].

2.5. FTIR Spectra of Metal Complexes

The FTIR spectral bands of the NB ligand and its complexes are shown in Table 2. The FTIR spectrum of free NB shows sharp bands at 1606 cm^{-1} and 1597 cm^{-1}, which were assigned to the stretching vibration of azomethine ν(-HC=N-) and benzothiazole imine ν(C=N), respectively. However, these bands may overlap with ν(C=C), which makes their complete interpretation difficult [18]. The nitro group of NB has two absorption bands at 1517 and 1337 cm^{-1}, which were assigned to asymmetric and symmetric vibrations of the NO_2 group [31]. The azomethine ν(-HC=N-) was shifted to a higher frequency upon complexation with metal ions. Moreover, the low-frequency regions of the spectra indicate the appearance of two weak-intensity bands in the range of 431 to 598 cm^{-1} in the FTIR spectra of the complexes, which were assigned to metal-nitrogen vibrations ν(M-N).

Table 2. FTIR main stretching absorption bands (cm^{-1}) of NB and its metal complexes.

Code	-HC=N-, Azomethine	-C=N-, Benzothiazole	C-NO_2	M-N	M-N
NB	1606	1597	1517, 1337		
Cu-NB	1637	1607	1528, 1344	500	442
Cd-NB	1630	1611	1505, 1340	474	431
Cr-NB	1639	1598	1522, 1342	576	536
Fe-NB	1643	1599	1573, 1307	598	537
Co-NB	1613	1576	1518, 1348	531	512

The FTIR spectral bands of the CB ligand and its complexes are shown in Table 3. The FTIR absorption bands at 1602 cm^{-1} and 1557 cm^{-1} in the spectrum of CB, which were assigned to the stretching vibration of azomethine ν(-HC=N-) and benzothiazole imine ν(C=N), respectively, were shifted to a higher frequency upon complexation with metal ions. Thus, the nitrogen atoms of CB are the coordination sites of metal complexes, as in the case of NB. The low-frequency regions of the spectra indicated the appearance of two weak-intensity bands in the range of 428 to 692 cm^{-1} in the FTIR spectra of the complexes, which were assigned to metal–nitrogen vibrations ν(M-N) [32].

Table 3. FTIR main stretching absorption bands (cm^{-1}) of CB and its metal complexes.

Code	-HC=N-, Azomethine	-C=N-, Benzothiazole	C-Cl	M-N	M-N
CB	1602	1557	755		
Cu-CB	1694	1603	758	653	631
Cr-CB	1612	1577	796	496	428
Fe-CB	1634	1598	712	620	600
Co-CB	1611	1576	795	692	649
Ni-CB	1693	1635	755	641	630

The FTIR spectral bands of HB and its complexes are shown in Table 4. The most distinguished feature of HB complexes is the shift of the azomethine ν(-HC=N-) bond at 1639 cm^{-1} to a lower frequency upon complexation with Co(II), Cu(II) and Ni(II) (Figure 1) in contrast to what was observed in the case of NB and CB. Yeap et al. observed a shift of the azomethine ν(-HC=N-) bond at 1638 cm^{-1} in HB to a lower frequency upon complexation with Cu(II) [18]. Furthermore, Salehi et al. reported similar shifts of the ν(-HC=N-) bond to a lower frequency upon complexation of (E)-2-(5-bromo-2-hydroxybenzylideneamino) phenol with Cu(II) and Ni(II) [33]. The common feature of these ligands may be the possible donation of phenolate groups to the metals, which enable the metal to exhibit backdonation to the C=N bond of azomethine. This backdonation is not possible for the high-charge Cr(III) and Fe(III) complexes with HB, which exhibit a shift of azomethine ν(-HC=N-) to a higher frequency as shown in Table 4.

Table 4. FTIR main stretching absorption bands (cm^{-1}) of HB and its metal complexes.

Code	-HC=N-, Azomethine	-C=N-, Benzothiazole	C-OH Phenolic	M-N	M-N
HB	1639	1604	1472, 1462		
Cu-HB	1620	1611	1489, 1475	598	428
Cd-HB	1632	1614	1485, 1423	552	442
Cr-HB	1647	1575	1485, 1423	558	496
Fe-HB	1644	1583	1488, 1428	527	494
Co-HB	1612	1584	1480, 1435	549	497
Ni-HB	1623	1613	1489, 1475	576	546

Intramolecular H-bonding is common in Schiff base compounds derived from aromatic aldehydes with a hydroxyl group in position 2 to the aldehyde group (Figure 2) [34]. Thus, the free HB ligand exhibited broad bands in the range of 2500 to 2800 cm^{-1} that can be ascribed to intramolecular (OH···N) H- bonding. These bands disappeared upon complexation with metal ions due to the involvement of O and N of HB in coordination with the metals. In their study of intramolecular hydrogen bonding in *N*-salicylideneaniline, Moosavi-Tekyeh and Dastani attributed the weak band between 2700 and 3100 cm^{-1}, which was sensitive to deuteration, to the OH group involved in strong intramolecular OH···N hydrogen bonding (in CCl_4 solvent) [35]. The higher-frequency broad bands at 3200–3500 cm^{-1} in HB can be attributed to the second phenolic OH group.

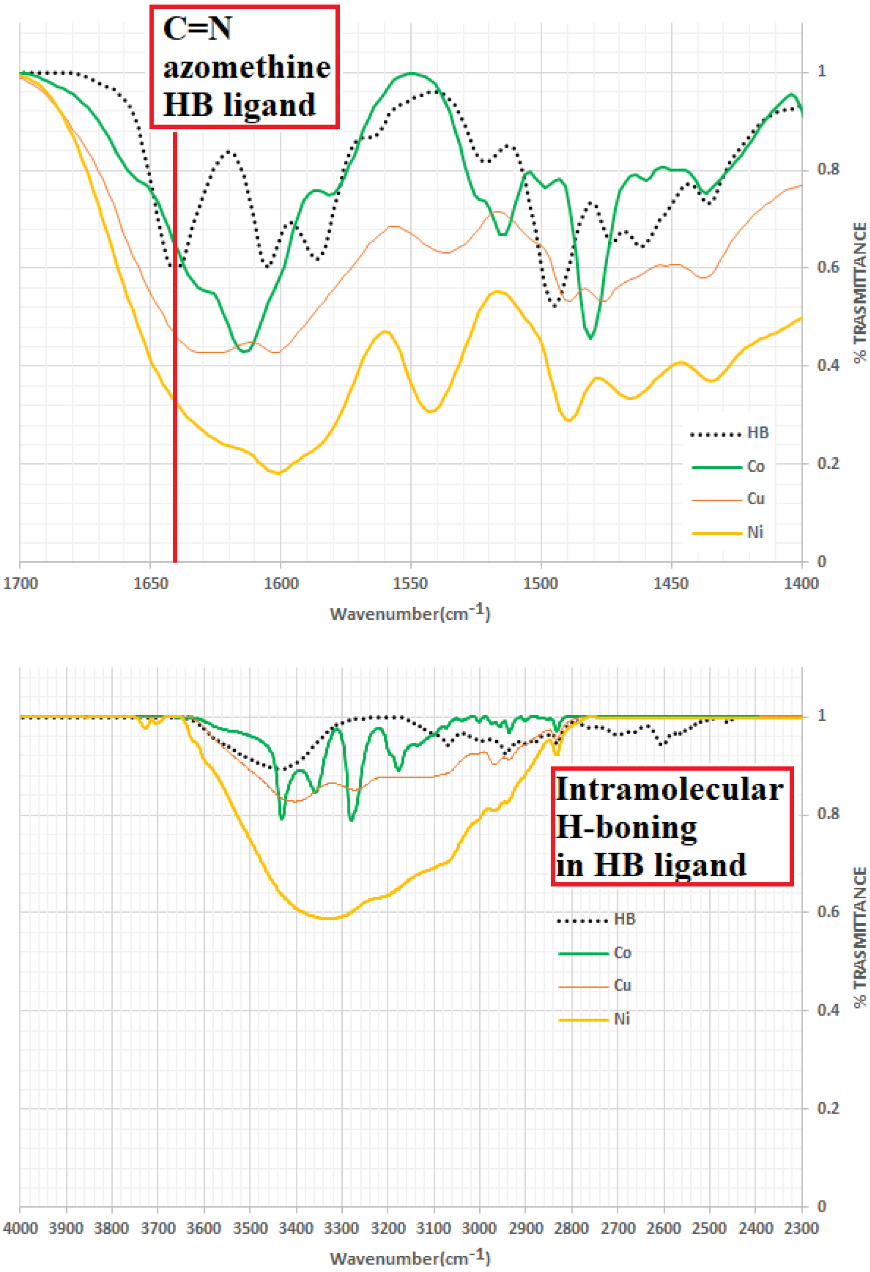

Figure 1. FTIR spectra of HB and its complexes with Cu, Co and Ni.

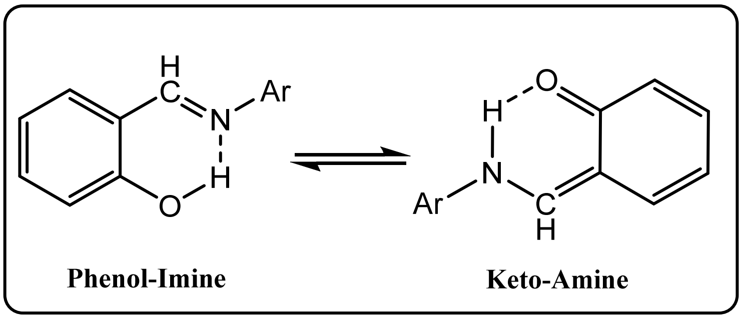

Figure 2. Intramolecular hydrogen bonding in the HB ligand.

2.6. ^{1}H-NMR Study of Complexes

Owing to the paramagnetic nature of Cu (II), Ni (II), Co (II), Fe (III) and Cr (III) complexes, the ^{1}H-NMR spectra were complicated, and it was not possible to follow the shifts exhibited by all the peaks of ligands upon complexation. However, the singlet peak of azomethine of NB at 9.44 ppm was shifted downfield (about 10.2 ppm, Figure S1 from Supplementary Materials) upon complexation with Cu, Cr and Cd (Table 5, Figures S2, S4 and S5). Similarly, the singlet peak of azomethine of the CB ligand at 9.44 ppm was shifted downfield (about 10.3 ppm, Figure S6) upon complexation with Cu, Cr and Ni (Table 5, Figures S7, S9 and S10), reflecting the fact azomethine nitrogen is the site of interaction. Furthermore, the singlet peak of azomethine of the HB ligand at 9.18 ppm (Figure S11) was shifted downfield (about 9.17 ppm) upon complexation with Cu and Cr (Table 5, Figures S12 and S14) and was not affected in the case of the Cd complex (Figure S13). The broad hydroxyl peaks of HB at 10.69 and 12.01 ppm exhibited a decrease in intensity and disappearance in the case of Cd and Cr complexes, respectively (Figures S13 and S14), indicating the involvement of hydroxyl groups in bonding. The sharpening of the hydroxyl groups in the Cu-HB complex reflects the decrease in intramolecular hydrogen bonding in HB upon complexation with Cu (Figure S12). The Cd-HB complex was partially dissociated in DMSO since the ^{1}H-NMR of the HB ligand (Figure S11) and Cd-HB (Figure S13) are almost identical, with more splitting of peaks in the case of the complex.

Table 5. Some ^{1}H-NMR peaks of NB, CB and HB and their metal complexes (ppm).

Code	-HC=N-, Azometh	CH_3-O	Code	-HC=N-, Azometh	CH_3-O	Code	-HC=N-, Azometh	CH_3-O	OH
NB	9.44	3.86	**CB**	9.44	3.86	**HB**	9.18	3.84	10.69, 12.01 (broad)
Cu-NB	10.24	3.84	**Cu-CB**	10.33	3.79	**Cu-HB**	9.91	3.61	10.61, 10.88 (sharp)
Cr-NB	10.25 9.20	3.76	**Cr-CB**	10.32	3.70	**Cr-HB**	9.94	3.78	disappeared
Cd-NB	10.22	3.76	**Ni-CB**	10.34	3.72	**Cd-HB**	9.17	3.84	10.68, 12.02 (broad, lower intensity)

Despite the paramagnetic nature of the complexes, some relatively sharp peaks were observed in the spectra of some complexes such as Cu-NB (Figure S2), Cu-CB (Figure S7) and Cu-HB (Figure S12). This may be due to the fact that some protons are far from the metal center, and they are outside the paramagnetic sphere of the metal. There are some examples in the literature that report similar observations where some peaks appear in the range of 0–10 ppm for paramagnetic complexes [36–38]. An alternative explanation may be that the DMSO solvent undergoes partial exchange with ligands, such as that reported for the ethylenediamine complex with Cu(II) [39].

Due to the high-spin configuration of Co(II) complexes, as shown by the magnetic susceptibility data (Section 2.4), the ^{1}H-NMR signals are expected to be spread over a wide range (-60 to 220 ppm [40] and -10 to 215 ppm [36]). Consequently, we believe that the Co-NB (Figure S3) and Co-CB (Figure S8) complexes are oxidized in air to Co(III) complexes, which is the reason for the noisy spectrum in the range of 0 to 11 ppm.

3. Materials and Methods

3.1. Materials and Instruments

The precursor 2-amino-6-methoxybenzothiazol,2-chlorebenzaldehyde, copper (II) chloride dihydrate, nickel (II) chloride hexahydrate and cobalt (II) chloride hexahydrate were obtained from Sigma-Aldrich. 2,4-Dihydroxybenzaldehyed, cadmium (II) chloride monohydrate and chromium (III) chloride hexahydrate were obtained from Acros Organics. 2-Nitrobenzaldehyde and iron (III) chloride hexahydrate were obtained from Fluka and Riedel-de Haën, respectively. Elemental analysis was carried out using an automated elemental analyzer EuroEA3000 (Euro Vector, Pavia, Italy). NMR spectra were recorded at room temperature by means of the AVANCE-III 400 MHz FT-NMR NanoBay spectrometer (Bruker, Fällanden, Switzerland) in dimethyl sulfoxide (DMSO-d_6) with tetramethyl silane (TMS) as an internal standard.

FTIR spectra were recorded using the Bruker Vertex 70-FT-IR Spectrometer (Bruker, Switzerland) using the KBr disc method in the region between 4000 and 400 cm^{-1}. Melting points were determined on the Stuart scientific melting apparatus (Stuart, UK). The magnetic susceptibility measurements were performed at room temperature (25 ± 2 °C) using a Johnson–Matthey balance (Johnson-Matthey Company, Germany). The effective magnetic moment (μeff) was calculated using (Equation (1)), where X_m is the molar magnetic susceptibility (m^3/mol) and T is the temperature (°C).

$$\mu\text{eff} = 2.84\sqrt{}\,(X_m\ T) \tag{1}$$

3.2. *Synthesis of Schiff Base Ligands*

The Schiff base ligands (NB, CB and HB) were prepared via the condensation of 2-amino-6-methoxybenzothiazol with 2-nitrobenzaldehyde, 2-chlorebenzaldehyde and 2,4-dihydroxybenzaldehyed, respectively (Scheme 1). A solution of aromatic aldehyde (5.548 mmol) in 30 mL of ethanol acidified with 3 drops of acetic acid was added to a solution of 2-Amino-6-methoxybenzothiazol (5.548 mmol) in 30 mL of ethanol. The reaction mixture was refluxed for 5 h and then concentrated by evaporating some of the solvent to precipitate the product, which was collected via suction filtration. The product was recrystallized using hot ethanol and dried at 60 °C in a vacuum oven. The nitro-, chloro- and hydroxy-substituted Schiff bases ligands are referred to as NB, CB and HB, respectively.

3.2.1. (E)-*N*-(6-methoxybenzo[d]thiazol-2-yl)-1-(2-nitrophenyl) methanimine (NB)

80% yield of an orange powder with melting point = 175–176 °C. Anal.Calcd for $C_{15}H_{11}N_3O_{S3}$ (%): C, 57.50; N, 13.41; H, 3.45; S, 10.23. found: C, 57.26; N, 13.26; H, 3.30; S, 10.00. FTIR data (KBr disc, cm^{-1}): 1606 ν(-HC=N- azomethine), 1560 ν(-C=N- benzothiazole), 1518, 1336 ν(-NO_2), 1227 ν(methoxy-O-CH_3). ^{1}H-NMR (400 MHz, DMSO-d_6) δ/ppm: 9.44 (s, 1H, azomethine -HC=N-), 8.28 (d, J^3 = 7.7 Hz, 1H), 8.20 (d, J^3 = 7.9 Hz, 1H), 7.97 – 7.84 (m, 3H), 7.71 (d, J^4 = 2.7 Hz, 1H), 7.16 (dd, J^3 J^4 = 8.9, 2.6 Hz, 1H), 3.87 (s, 3H, methoxy-O-CH_3). ^{13}C NMR (100 MHz, DMSO-d_6) δ/ppm: 168.38 (-C=N- benzothiazole), 163.13 (azomethine -HC=N-), 158.11, 150.13, 145.95, 136.26, 134.53, 133.78, 130.30, 129.33, 125.38, 124.24, 116.69 and 105.61 were assigned to the aromatic carbons, 56.24 (-O-CH_3). The assignment of all ^{1}H and ^{13}C-NMR chemical shifts of the NB ligand was accomplished via the assistance of 2D-NMRm which include COSY, HMQC and HMBC experiments (Table S1 and Figures S15–S17).

3.2.2. (E)-1-(2-chlorophenyl)-*N*-(6-methoxybenzo[d]thiazol-2-yl) methanimine (CB)

86% yield of a yellow powder with m.p = 122–124 °C. Anal.Calcd for $C_{15}H_{11}ClN_2OS$ (%): C, 59.50; N, 9.25; H, 3.66; S, 10.59. found: C, 59.26; N, 9.15; H, 3.40; S, 10.21. FTIR data (KBr disc, cm^{-1}): 1606 ν (azomethine -HC=N-), 1550 ν(-C=N- benzothiazole), 1273 ν(methoxy -O-CH_3), 755 ν(C-Cl). ^{1}H NMR (400 MHz, DMSO-d6) δ/ppm: 9.44 (s, 1H, azomethine -HC=N-), 8.26 (d, J^3 = 7.7 Hz, 1H), 7.90 (d, J^3 = 8.9 Hz, 1H), 7.71 – 7.65 (m, 3H), 7.61 – 7.50 (m, 1H), 7.15 (dd, J^3 J^4 = 8.9, 2.7 Hz, 1H), 3.86 (s, 3H, methoxy-O-CH_3). ^{13}C NMR (100 MHz, DMSO-d_6) δ/ppm: 168.82 (-C=N- benzothiazole), 161.63 (azomethine -HC=N-), 157.96, 145.96, 136.85, 136.38, 135.18, 131.79, 130.95, 129.45, 128.48, 124.14, 116.62 and 105.56 were attributed to the aromatic carbons, 56.23(-O-CH_3).

3.2.3. (E)-4-(((6-methoxybenzo[d]thiazol-2-yl)imino) methyl) benzene-1,3-diol (HB)

85% yield of a yellow powder with m.p = 214-216 (dec) °C. Anal.Calcd for $C_{15}H_{12}N_2O_{S3}$, (%): C, 59.99; N, 9.33; H, 4.03; S, 10.68. found: C, 59.82; N, 9.26; H, 3.99; S, 10.48. FTIR data (KBr disc, $cm^{-1)}$: 1640 ν(azomethine -HC=N-), 1603 ν(-C=N- imine BTA), 1493,1455 ν(phenolic -C-OH), 1248 ν(methoxy -O-CH_3). ^{1}H NMR (400 MHz, DMSO-d_6) δ/ppm: 12.01 (s, 1H, OH), 10.69 (s, 1H, OH), 9.18 (s, 1H, azomethine -HC=N-), 7.79 (d, J^3 = 8.9 Hz, 1H), 7.72 (d, J^3 = 8.6 Hz, 1H), 7.63 (d, J^4 = 2.6 Hz, 1H), 7.09 (dd, J^3J^4 = 8.9, 2.6 Hz, 1H), 6.47 (dd, J^3J^4 = 8.6, 2.2 Hz, 1H), 6.38 (d, J^4 = 2.3 Hz, 1H), 3.84 (s, 3H, methoxy-O-CH_3). ^{13}C NMR (100 MHz, DMSO-d_6) δ/ppm: 168.35 (-C=N- benzothiazole), 165.27 (azomethine -HC=N-), 165.18 (phenolic -C-OH), 163.69 (phenolic -C-OH), 157.56, 145.97, 135.30, 134.76, 123.30, 116.62, 112.37, 109.80, 105.56, 102.89, which were ascribed to the aromatic carbons; 56.18 (-O-CH_3). The assignment of all ^{1}H and ^{13}C-NMR chemical shifts was verified using 2D-NMR, which include COSY, HMQC and HMBC experiments (Table S1 and Figures S18–S20)

All organic reactions were monitored by thin-layer chromatography (TLC) silica gel sheet, F_{254}; 20 cm × 20 cm (Merk Aluminum, Germany) and detected by visualization of the sheet under a UV lamp (354 nm).

3.3. Synthesis of Metal Complexes

3.3.1. Synthesis of NB Complexes

The NB complexes were prepared by dissolving 0.33 mmol of the metal salt ($CuCl_2$ $2H_2O$, $NiCl_2$ $6H_2O$, $CoCl_2$ $6H_2O$, $CdCl_2$ H_2O, $CrCl_3$ $6H_2O$, $FeCl_3$ $6H_2O$) in 5.0 mL of ethanol and dissolving 0.66 mmol of the NB ligand in 40 mL of hot ethanol (50 °C), mixing the two solutions and refluxing for 1 h. Then the solvent was partially evaporated to half of its volume until obtaining a precipitate, which was collected after suction filtration, washing with ethanol, and drying in a vacuum oven at 60 °C.

The yield, color and elemental analysis data for NB complexes are summarized as follows:

- Cu-NB: Yield: 58%, color: Dark green, m.p.: 195–197 °C, analysis: C 46.87, H 2.87, N 10.89, S 8.21%, calculated for CuL_2Cl_2 $0.5H_2O$: C 46.76, H 3.01, N 10.91, S 8.33%.
- Cd-NB: Yield: 64%, color: Orange, m.p.: 292–294 °C (dec), analysis: C 44.98, H 2.95, N 10.78, S 8.01%, calculated for $CdL_2Cl(OH)$ $0.5H_2O$: C 45.01, H 3.02, N 10.50, S 8.01%.
- Cr-NB: Yield: 66%, color: Dark green, m.p.: 70–72 °C, analysis: C 48.67, H 3.30, N 11.52, S 8.78%, calculated for $CrL_2(OH)_3$ $0.5H_2O$: C 48.78, H 3.55, N 11.38, S 8.68%.
- Fe-NB: Yield: 57%, color: Brown, m.p.: 134–136 °C, analysis: C 47.98, H 3.11, N 11.85, S 8.89%, calculated for $FeL_2Cl(OH)_2$: C 47.92, H 3.22, N 11.18, S 8.53%.
- Co-NB: Yield: 62%, color: Blue, m.p.: 285–287 °C, analysis: C 47.87, H 3.27, N 11.45, S 8.89%, calculated for $CoL_2Cl(OH)$ $0.5H_2O$: C 48.23, H 3.24, N 11.25, S 8.58%.

3.3.2. Synthesis of CB Complexes

The CB complexes were prepared by dissolving 0.33 mmol of the metal salt ($CuCl_2$ $2H_2O$, $NiCl_2$ $6H_2O$, $CoCl_2$ $6H_2O$, $CdCl_2$ H_2O, $CrCl_3$ $6H_2O$, $FeCl_3$ $6H_2O$) in 5.0 mL of ethanol and dissolving 0.66 mmol of the CB ligand in 25 mL of hot ethanol (50 °C), mixing the two solutions and refluxing for 1 h. Then the solvent was partially evaporated to half of its volume until obtaining a precipitate, which was collected after suction filtration, washing with ethanol and drying in a vacuum oven at 60 °C.

The yield, color and elemental analysis data for CB complexes are summarized as follows:

- Cu-CB: Yield: 55%, color: Dark green, m.p.: 53–55 °C, analysis: C 48.89, H 2.91, N 7.89, S 8.81%, calculated for CuL_2Cl_2: C 48.69, H 3.00, N 7.57, S 8.67%.
- Cr-CB: Yield: 62%, color: Blue, m.p.: 278–280 °C (dec.), analysis: C 49.85, H 3.54, N 7.75, S 8.78%, calculated for $CrL_2Cl(OH)_2$: C 49.56, H 3.33, N 7.71, S 8.82%.
- Fe-CB: Yield: 57%, color: Black, m.p.: 88–90 °C, analysis: C 49.87, H 3.60, N 7.96, S 8.97%, calculated for $FeL_2(OH)_3$ $0.5H_2O$: C 49.95, H 3.63, N 7.77, S 8.89%.
- Co-CB: Yield: 55%, color: Navy-blue, m.p.: 285–287 °C, analysis: C 49.60, H 3.22, N 7.75, S 8.98%, calculated for $CoL_2Cl(OH)$ $0.5H_2O$: C 49.63, H 3.33, N 7.72, S 8.83%.
- Ni-CB: Yield: 54%, color: Green, m.p.: 228–230 °C, analysis: C 48.88, H 2.89, N 7.47, S 8.35%, calculated for NiL_2Cl_2: C 49.01, H 3.02, N 7.62, S 8.72%.

3.3.3. Synthesis of HB Complexes

The HB complexes were prepared by dissolving 0.33 mmol of the metal salt ($CuCl_2$ $2H_2O$, $NiCl_2$ $6H_2O$, $CoCl_2$ $6H_2O$, $CdCl_2$ H_2O, $CrCl_3$ $6H_2O$, $FeCl_3$ $6H_2O$) in 5.0 mL of ethanol and dissolving 0.66 mmol of the HB ligand in 50 mL of hot ethanol (60 °C), mixing the two solutions and refluxing for 1 h. Then the solvent was partially evaporated to half of its volume until obtaining a precipitate, which was collected after suction filtration, washing with ethanol and drying in a vacuum oven at 60 °C.

The yield, color and elemental analysis data for HB complexes are summarized as follows:

- Cu-HB: Yield: 68%, color: Dark green, m.p.: 93–95 °C, analysis: C 49.50, H 3.54, N 7.91, S 8.41%, calculated for $CuL_2Cl(OH)$ $0.5H_2O$: C 49.65, H 3.61, N 7.72, S 8.84%.
- Cd-HB: Yield: 59%, color: Yellow, m.p.: 270–272 °C (dec.), analysis: C 46.23, H 3.21, N 7.25, S 8.56%, calculated for $CdL_2Cl(OH)$ $0.5H_2O$: C 46.52, H 3.38, N 7.23, S 8.28%.
- Cr-HB: Yield: 66%, color: Reddish-brown, m.p.: 92–94 °C, analysis: C 49.75, H 3.87, N 7.51, S 9.12%, calculated for $CrL_2Cl(OH)_2$: C 49.90, H 3.63, N 7.76, S 8.88%.
- Fe-HB: Yield: 67%, color: Black, m.p.: 95–97 °C, analysis: C 49.87, H 3.64, N 7.88, S 8.91%, calculated for $FeL_2Cl(OH)_2$: C 49.63, H 3.61, N 7.72, S 8.83%.
- Co-HB: Yield: 63%, color: Green, m.p.: 110–112 °C (dec.), analysis: C 49.89, H 3.81, N 8.01, S 9.11%, calculated for $CoL_2Cl(OH)$ $0.5H_2O$: C 49.97, H 3.63, N 7.77, S 8.89%.
- Ni-HB: Yield: 66%, color: Reddish-green, m.p.: 190–192 °C (dec.), analysis: C 49.04, H 3.11, N 7.27, S 8.20%, calculated for NiL_2Cl_2: C 49.34, H 3.31, N 7.67, S 8.78%.

4. Conclusions

Based on the values of magnetic susceptibility elemental analysis of complexes of NB, CB and HB with Cu(II), Cd(II), Co(II) and Ni(II), octahedral $[ML_2Cl_2]$ and $[ML_2Cl(OH)]$ structures were suggested where the ligand (L:NB, CB or HB) is bidentate through the nitrogen atoms of azomethine and benzothiazole. In the Cr(III) and Fe(III) complexes, octahedral $ML_2Cl(OH)_2$ or $ML_2(OH)_3$ structures were proposed in which one ligand is monodentate and the other is bidentate. The nitro- (NB) and chloro- (CB) substituted Schiff base ligands exhibited different FTIR and NMR spectroscopic behavior from the electron-donating OH-substituted (HB) ligand. The azomethine ν(-HC=N-) and ^{1}H-NMR peaks of NB and CB were shifted to a higher frequency and downfield, respectively, upon complexation with Co(II), Ni(II), Cu(II), Cd(II), Cr(III) and Fe(III). The bonding of OH groups of HB to Co(II), Cu(II) and Ni(II) enables π-backdonation from these metals to the azomethine of Schiff bases and a consequent shift of ν(-HC=N-) to a lower frequency and changes in the intensity of the ^{1}H-NMR peak of OH.

Supplementary Materials: The following supporting information can be downloaded at: https://www.mdpi.com/article/10.3390/inorganics10040043/s1.

Author Contributions: Conceptualization, M.S. (Mahmoud Sunjuk) and M.S. (Majed Shtaiwi); methodology, L.A.-N.; software, L.A.-N.; validation, L.A.-E., M.S. (Mahmoud Sunjuk) and M.S. (Majed Shtaiwi); formal analysis, L.A.-N.; investigation, M.S. (Majed Shtaiwi), K.S. and B.E.-E.; resources, L.A.-N.; data curation, M.A.-N., L.A.-E. and L.A.-N.; writing—original draft preparation, B.E.-E., K.S. and L.A.-E.; writing—review and editing, B.E.-E., K.S., L.A.-N., L.A.-E.; visualization, M.A.-N. and L.A.-N.; supervision, M.S. (Majed Shtaiwi), B.E.-E.; project administration, M.S. (Mahmoud Sunjuk) and M.S. (Majed Shtaiwi); funding acquisition, M.S. (Mahmoud Sunjuk). All authors have read and agreed to the published version of the manuscript.

Funding: This research received no external funding.

Data Availability Statement: All data is available in this manuscript or the supporting information.

Conflicts of Interest: The authors declare no conflict of interest.

References

1. Schiff, H. Mittheilungen aus dem Universitätslaboratorium in Pisa: Eine neue Reihe organischer Basen. *Justus Liebigs Ann. Chem.* **1864**, *131*, 118–119. [CrossRef]
2. Da Silva, C.M.; da Silva, D.L.; Modolo, L.V.; Alves, R.B.; de Resende, M.A.; Martins, C.V.B.; de Fátima, Â. Schiff bases: A short review of their antimicrobial activities. *J. Adv. Res.* **2011**, *2*, 1–8. [CrossRef]
3. Kajal, A.; Bala, S.; Kamboj, S.; Sharma, N.; Saini, V. Schiff bases: A versatile pharmacophore. *J. Catal.* **2013**, *2013*, 893512. [CrossRef]
4. Altamimi, M.A.; Hussain, A.; Alshehri, S.; Imam, S.S.; Alnami, A.; Bari, A. Novel Hemocompatible Imine Compounds as Alternatives for Antimicrobial Therapy in Pharmaceutical Application. *Processes* **2020**, *8*, 1476. [CrossRef]
5. Abdel-Rahman, L.H.; El-Khatib, R.M.; Nassr, L.A.; Abu-Dief, A.M.; Lashin, F.E.-D. Design, characterization, teratogenicity testing, antibacterial, antifungal and DNA interaction of few high spin Fe (II) Schiff base amino acid complexes. *Spectrochim. Acta Part A Mol. Biomol. Spectrosc.* **2013**, *111*, 266–276. [CrossRef]
6. Dehkhodaei, M.; Sahihi, M.; Rudbari, H.A. Spectroscopic and molecular docking studies on the interaction of Pd (II) & Co (II) Schiff base complexes with β-lactoglobulin as a carrier protein. *J. Biomol. Struct. Dyn.* **2018**, *36*, 3130–3136.
7. Abdel-Rahman, L.H.; Ismail, N.M.; Ismael, M.; Abu-Dief, A.M.; Ahmed, E.A.-H. Synthesis, characterization, DFT calculations and biological studies of Mn (II), Fe (II), Co (II) and Cd (II) complexes based on a tetradentate ONNO donor Schiff base ligand. *J. Mol. Struct.* **2017**, *1134*, 851–862. [CrossRef]
8. Kostova, I.; Saso, L. Advances in research of Schiff-base metal complexes as potent antioxidants. *Curr. Med. Chem.* **2013**, *20*, 4609–4632. [CrossRef]
9. Xavier, A.; Srividhya, N. Synthesis and study of Schiff base ligands. *IOSR J. Appl. Chem.* **2014**, *7*, 6–15. [CrossRef]
10. Yousif, E.; Majeed, A.; Al-Sammarrae, K.; Salih, N.; Salimon, J.; Abdullah, B. Metal complexes of Schiff base: Preparation, characterization and antibacterial activity. *Arab. J. Chem.* **2017**, *10*, S1639–S1644. [CrossRef]
11. Vadivel, T.; Dhamodaran, M. Synthesis, characterization and antibacterial studies of ruthenium (III) complexes derived from chitosan Schiff base. *Int. J. Biol. Macromol.* **2016**, *90*, 44–52. [CrossRef]
12. Keri, R.S.; Patil, M.R.; Patil, S.A.; Budagumpi, S. A comprehensive review in current developments of benzothiazole-based molecules in medicinal chemistry. *Eur. J. Med. Chem.* **2015**, *89*, 207–251. [CrossRef]
13. Liu, X.; Dong, Z.-B. A Review on Domino Condensation/Cyclization Reactions for the Synthesis of 2-Substituted 1, 3-Benzothiazole Derivatives. *Eur. J. Org. Chem.* **2020**, *2020*, 408–419. [CrossRef]
14. Mishra, V.R.; Ghanavatkar, C.W.; Mali, S.N.; Chaudhari, H.K.; Sekar, N. Schiff base clubbed benzothiazole: Synthesis, potent antimicrobial and MCF-7 anticancer activity, DNA cleavage and computational study. *J. Biomol. Struct. Dyn.* **2019**, *38*, 1772–1785. [CrossRef]
15. El-Dakdouki, M.H.; Hussein, A.; Abdallah, H.; Shatila, R.; Mouneimne, Y. Synthesis of novel 2H-indazole analogues via the Davis-Beirut reaction and conjugation onto magnetic nanoparticles. *Tetrahedron* **2017**, *73*, 5769–5777. [CrossRef]
16. Li, W.; Song, B.; Bhadury, P.S.; Li, L.; Wang, Z.; Zhang, X.; Hu, D.; Chen, Z.; Zhang, Y.; Bai, S.; et al. Chiral cinchona alkaloid-derived thiourea catalyst for enantioselective synthesis of novel β-amino esters by mannich reaction. *Chirality* **2012**, *24*, 223–231. [CrossRef]
17. Li, W.; Wang, Y.; Xu, D. Asymmetric Synthesis of α-Amino Phosphonates by Using Cinchona Alkaloid-Based Chiral Phase Transfer Catalyst. *Eur. J. Org. Chem.* **2018**, *2018*, 5422–5426. [CrossRef]
18. Yeap, G.-Y.; Heng, B.-T.; Faradiana, N.; Zulkifly, R.; Ito, M.M.; Tanabe, M.; Takeuchi, D. Synthesis, molecular structures and phase transition studies on benzothiazole-cored Schiff bases with their Cu(II) and Pd(II) complexes: Crystal structure of (E)-6-methoxy-2-(4-octyloxy-2-hydroxybenzylideneamino)benzothiazole. *J. Mol. Struct.* **2012**, *1012*, 1–11. [CrossRef]
19. Ha, S.-T.; Koh, T.-M.; Yeap, G.-Y.; Lin, H.-C.; Lee, S.-L.; Win, Y.-F.; Ong, S.-T. Synthesis and Mesomorphic Properties of 6-Methoxy- and 6-Ethoxy-2-(2-Hydroxy-4 Alkanoyloxybenzylidenamino)Benzothiazoles. *Mol. Cryst. Liq. Cryst.* **2010**, *528*, 10–22. [CrossRef]
20. Chohan, Z.H.; Supuran, C.T. Antibacterial Zn (II) compounds of. Schiff bases derived from some benzothiazoles. *Main Group Met. Chem.* **2002**, *25*, 291–296.
21. Chohan, Z.H. Biologically active transition metal chelates of Ni (ll), Cu (ll) AND Zn (ll) with 2-aminothiazole-derived Schiff-bases: Their synthesis, characterization and the role of anions (NO_3, SO-, C_2O_4 and CH_3CO_2) on their antibacterial properties. *Met.-Based Drugs* **1999**, *6*, 3.
22. Kettle, S.F.A. *Physical Inorganic Chemistry: A Coordination Chemistry Approach*; Springer: Berlin/Heidelberg, Germany, 1996; Chapter 9.
23. Angelusiu, M.V.; Barbuceanu, S.-F.; Draghici, C.; Almajan, G.L. New Cu (II), Co (II), Ni (II) complexes with aroyl-hydrazone based ligand. Synthesis, spectroscopic characterization and in vitro antibacterial evaluation. *Eur. J. Med. Chem.* **2010**, *45*, 2055–2062. [CrossRef] [PubMed]
24. Housecroft, C.E.; Sharpe, A.G. *Inorganic Chemistry*; Pearson Education Limited England: London, UK, 2005; p. 583.
25. Dalal, M. *A Textbook of Inorganic Chemistry—Volume 1*; Dalal Institute: Haryana, India, 2019; Chapter 9.
26. Willis, J.B.; Mellor, D.P. The Magnetic Susceptibility of Some Nickel Complexes in Solution. *J. Am. Chem. Soc.* **1947**, *69*, 1237–1240. [CrossRef]
27. Blanchard, S.; Neese, F.; Bothe, E.; Bill, E.; Weyhermüller, T.; Wieghardt, K. Square Planar vs Tetrahedral Coordination in Diamagnetic Complexes of Nickel(II) Containing Two Bidentate π-Radical Monoanions. *Inorg. Chem.* **2005**, *44*, 3636–3656. [CrossRef]

28. Tripathi, S.; Dey, A.; Shanmugam, M.; Narayanan, R.S.; Chandrasekhar, V. Cobalt(II) Complexes as Single-Ion Magnets. In *Organometallic Magnets*; Topics in Organometallic Chemistry; Springer: Cham, Switzerland, 2018; Volume 64. [CrossRef]
29. Emara, A.A.; El-Sayed, B.A.; Ahmed, E.-S.A. Syntheses, spectroscopic characterization and thermal behavior on novel binuclear transition metal complexes of hydrazones derived from 4, 6-diacetylresorcinol and oxalyldihydrazine. *Spectrochim. Acta Part A Mol. Biomol. Spectrosc.* **2008**, *69*, 757–769. [CrossRef]
30. Tarafder, M.T.H.; Kasbollah, A.; Crouse, K.A.; Ali, A.M.; Yamin, B.M.; Fun, H.-K. Synthesis and characterization of Zn (II) and Cd (II) complexes of S-benzyl-β-*N*-(2-pyridyl) methylenedithiocarbazate (HNNS): Bioactivity of the HNNS Schiff base and its Zn (II), Cu (II) and Cd (II) complexes and the X-ray structure of the [Zn (NNS) 2] complex. *Polyhedron* **2001**, *20*, 2363–2370.
31. Kross, R.D.; Fassel, V.A. The Infrared Spectra of Aromatic Compounds. IV. The Nitro Valence Vibrations in p-Disubstituted Nitrobenzenes1. *J. Am. Chem. Soc.* **1956**, *78*, 4225–4229. [CrossRef]
32. Alkuubaisi, H.M.; Sallom, H.K.; Kadim, W.H.; Shaker, S.H. Synthesis and Characterization of Co(II),Ni(II),Cu(II) and Zn(II) Complexes with Benzothiazol-2-yl-(4-chloro-benzylidene)-amine. *IOSR J. Appl. Chem.* **2016**, *9*, 11–16. [CrossRef]
33. Salehi, M.; Faghani, F.; Kubicki, M.; Bayat, M. New complexes of Ni(II) and Cu(II) with tridentate ONO Schiff base ligand: Synthesis, crystal structures, electrochemical and theoretical investigation. *J. Iran. Chem. Soc.* **2018**, *15*, 2229–2240. [CrossRef]
34. Gavranić, M.; Kaitner, B.; Meštrović, E. Intramolecular N- H... O hydrogen bonding, quinoid effect, and partial π-electron delocalization in *N*-aryl Schiff bases of 2-hydroxy-1-naphthaldehyde: The crystal structures of planar *N*-(α-naphthyl)-and *N*-(β-naphthyl)-2-oxy-1-naphthaldimine. *J. Chem. Crystallogr.* **1996**, *26*, 23–28. [CrossRef]
35. Moosavi-Tekyeh, Z.; Dastani, N. Intramolecular hydrogen bonding in *N* salicylideneaniline: FT-IR spectrum and quantum chemical calculations. *J. Mol. Struct.* **2015**, *1102*, 314–322. [CrossRef]
36. Pankratova, Y.; Aleshin, D.; Nikovskiy, I.; Novikov, V.; Nelyubina, Y. In Situ NMR Search for Spin-Crossover in Heteroleptic Cobalt(II) Complexes. *Inorg. Chem.* **2020**, *59*, 7700–7709. [CrossRef] [PubMed]
37. Ramadan, S.; Hambley, T.W.; Kennedy, B.J.; Lay, P.A. NMR Spectroscopic Characterization of Copper(II) and Zinc(II) Complexes of Indomethacin. *Inorg. Chem.* **2004**, *43*, 2943–2946. [CrossRef]
38. Nanthakumar, A.; Fox, S.; Murthy, N.N.; Karlin, K.D. Inferences from the 1H-NMR Spectroscopic Study of an Antiferromagnetically Coupled Heterobinuclear Fe(III)−(X)−Cu(II) $S = 2$ Spin System (X = O^{2-}, OH^{-}). *J. Am. Chem. Soc.* **1997**, *119*, 3898–3906. [CrossRef]
39. Watkins, C.L.; Vigee, G.S. Ethylenediamine complexes of copper(II) and nickel(II) in solutions of dimethyl sulfoxide. *J. Phys. Chem.* **1976**, *80*, 83–88. [CrossRef]
40. Valencia, M.N.C.; Corrales, H.F.Z.; Martínez, G. Electronic and electrochemical properties of grid-type metal ion complexes (Fe^{2+} and Co^{2+} with a pyridine-pyrimidine-pyridine based bis(hydrazone). *Rev. Colomb. Quím.* **2018**, *47*, 45–53. [CrossRef]